

## Supporting Information

### Controlled chiral arrangement of silver nanoparticles in supramolecular gels modulated by cooling rate

Rong Wang,<sup>a</sup> Jiayi Cui,<sup>b</sup> Xinhua Wan\*<sup>a</sup> and Jie Zhang\*<sup>a</sup>

- a. Beijing National Laboratory for Molecular Science, Key Laboratory of Polymer Chemistry and Physics of Minister of Education, Center for Soft Matter Science and Engineering, College of Chemistry and Molecular Engineering, Peking University, Beijing 100871, China.  
b. INM-Leibniz Institute for New Materials, Campus D22, 66123, Saarbrücken, Germany.

\*To whom correspondence should be addressed.

E-mail: xhwan@pku.edu.cn (X. H. W.) and jz10@pku.edu.cn (J. Z.)

#### Experimental Section

Silver nitrate (>99.0%) was purchased from Beijing Coupling Technology Co. Ltd. Keggin POMs ( $H_4[SiW_{12}O_{40}]$ ) was purchased from Sinopharm Chemical Reagent Co. Ltd. And *L*-(-)-Glucose (Macklin) was purchased from Baoluyi (Beijing) biotechnology Co. Ltd. All the reagents were used as received.

#### Characterization.

<sup>1</sup>H NMR (400 MHz) were recorded on a Bruker Avance III spectrometer at room temperature with the internal standard of TMS. UV-Vis absorption spectra were carried on a Lambda 35 UV-Vis spectrometer. CD spectra were performed on a Jasco J-810 circular dichroism spectrometer using a circular quartz cell with a length of 0.2mm. TEM images were recorded from a JEOL JEM-2100 (Japan) transmission electron microscopy operated at 200kV. Samples were prepared by laying a few amount gel onto copper grids coated with amorphous membranes, and then removing after 1min, and finally freeze drying. SEM images were recorded with the Hitachi S-4800 with the acceleration voltage of 2Kv and an 8mm working distance. All samples were prepared by laying a few mount of gel onto fresh silicon wafer, and then removing after 1min, and finally drying in air. Photoreduction of AgNO<sub>3</sub> was performed by using a lamp (HSX-F/UV 300) with a 300nm polarizing film.

**Preparation of geltor D-C4TG (4''-butoxy-4-hydroxy-p-terphenyl-β-D-glucoside).** D-C4TG was synthesized according to literature procedure.<sup>1</sup>

**Preparation of geltor L-C4TG (4''-butoxy-4-hydroxy-p-terphenyl-β-L-glucoside).** The synthesis of L-C4TG was similar to that of D-C4TG, expect D-glucose was replaced by L-glucose. <sup>1</sup>H NMR (400 MHz, DMSO-d<sub>6</sub>, δ ppm): 7.75-7.57 (m, 8H, p-terphenyl), 7.18-7.06 (d, 2H, p-terphenyl), 7.06-6.97 (d, 2H, p-terphenyl), 4.94-4.86 (d, 1H, H-1), 4.07-3.96 (t, 2H, OCH<sub>2</sub>CH<sub>2</sub>CH<sub>2</sub>CH<sub>3</sub>), 3.76-3.65 (d, 1H, H-6a), 3.53-3.43 (dd, 1H, H-6b), 3.40-3.35 (m, 1H, H-5), 3.30-3.23 (m, 2H, H-3 and H-4), 3.21-3.11 (t, 1H, H-2), 1.78-1.66 (m, 2H, OCH<sub>2</sub>CH<sub>2</sub>CH<sub>2</sub>CH<sub>3</sub>), 1.52-1.39 (m, 2H, OCH<sub>2</sub>CH<sub>2</sub>CH<sub>2</sub>CH<sub>3</sub>), 1.00-0.88 (t, 3H, OCH<sub>2</sub>CH<sub>2</sub>CH<sub>2</sub>CH<sub>3</sub>).

**Preparation of supramolecular gels.** In a typical experiment, 2mg/ml C4TG hot solution was prepared in the mixture H<sub>2</sub>O/1,4-dioxane (40/60 v/v) at 85°C for 15min. Then 10mg POMs and 2.95mg AgNO<sub>3</sub> were added to the above hot solution. After mixing uniformly, hot solution was allowed to cool down to room temperature through RC and SC process, respectively. In RC process, gel was obtained by allowing hot solution to cool down to room temperature immediately; while in SC process, gel was obtained by allowing hot isotropic solution to cool down to room temperature at a rate of 1°C/min. Then, the AgNO<sub>3</sub> was in situ reduced after the irradiation of UV light. A circular quartz cell with a length of 0.2mm was used for *in-situ* preparation of Ag NPs, and then for CD and UV-Vis spectroscopy measurement.

**Mathematical fitting of CD spectra.** Mathematical fitting was carried out using OriginPro 8.5 package. Selected two functions to fit two peaks which represented two different chiral sources. Continually changed parameters, such as the function type, wavelength range and half peak width, until satisfying fitting coefficient has been achieved.

### Supplementary Figures and Tables

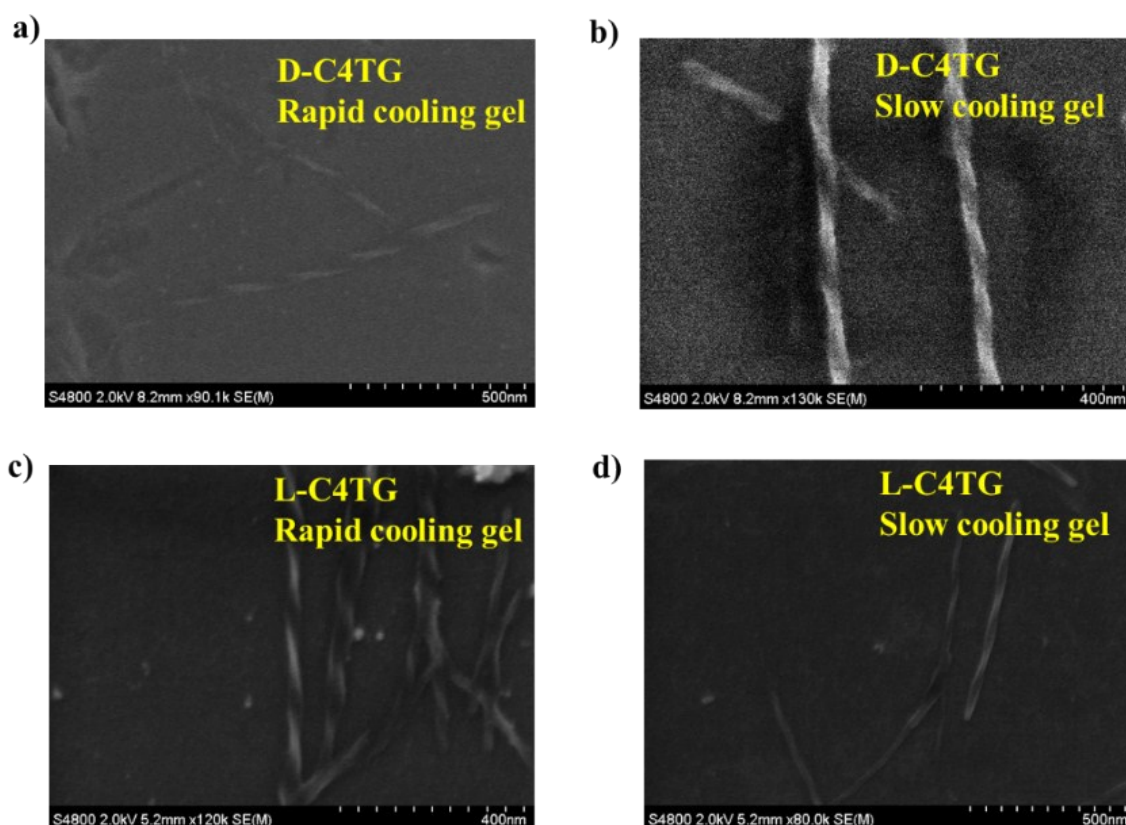


**Fig. S1** SEM images of D-C4TG hybrid gel before UV irradiation in RC process (a) and in SC process (b), and L-C4TG hybrid gel before UV irradiation in RC process (c) and in SC process (d).

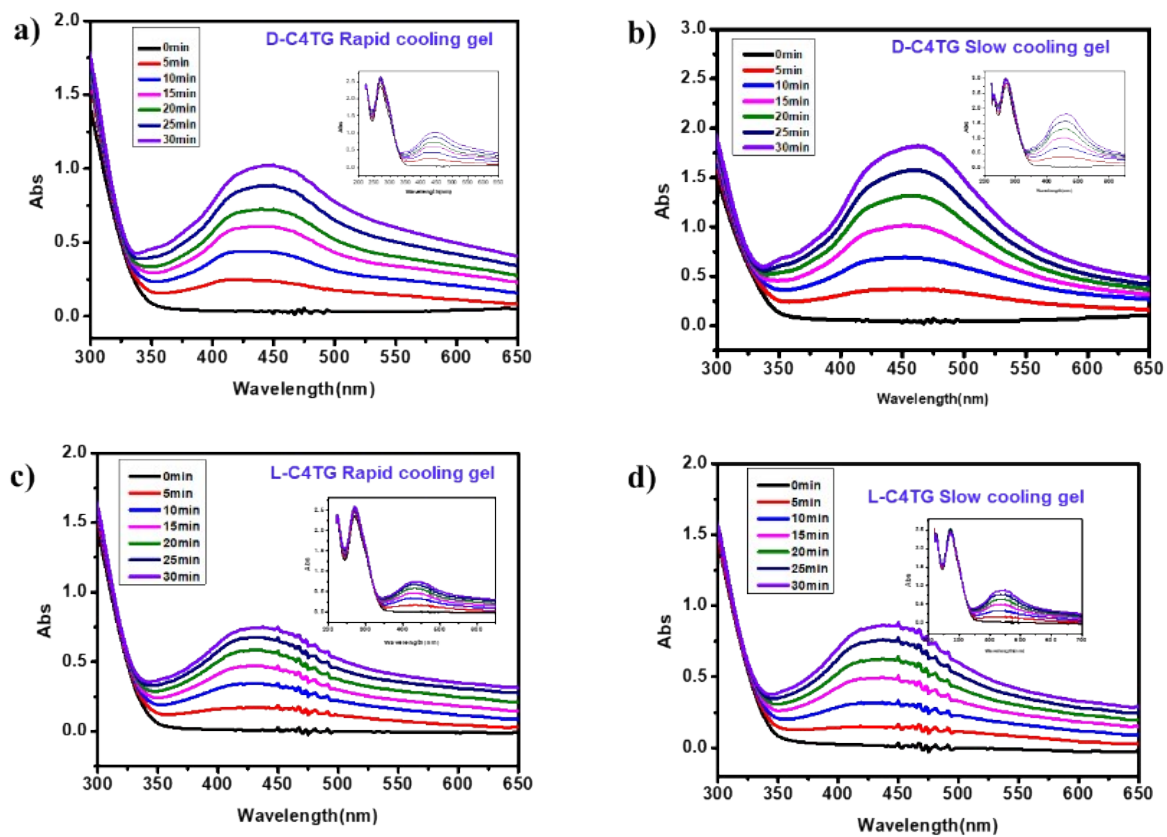


**Fig. S2** UV-Vis absorption spectra of D-C4TG hybrid material in RC process (a) and in SC process (b), and L-C4TG hybrid material in RC process (c) and in SC process (d) after increasing durations of UV irradiation.

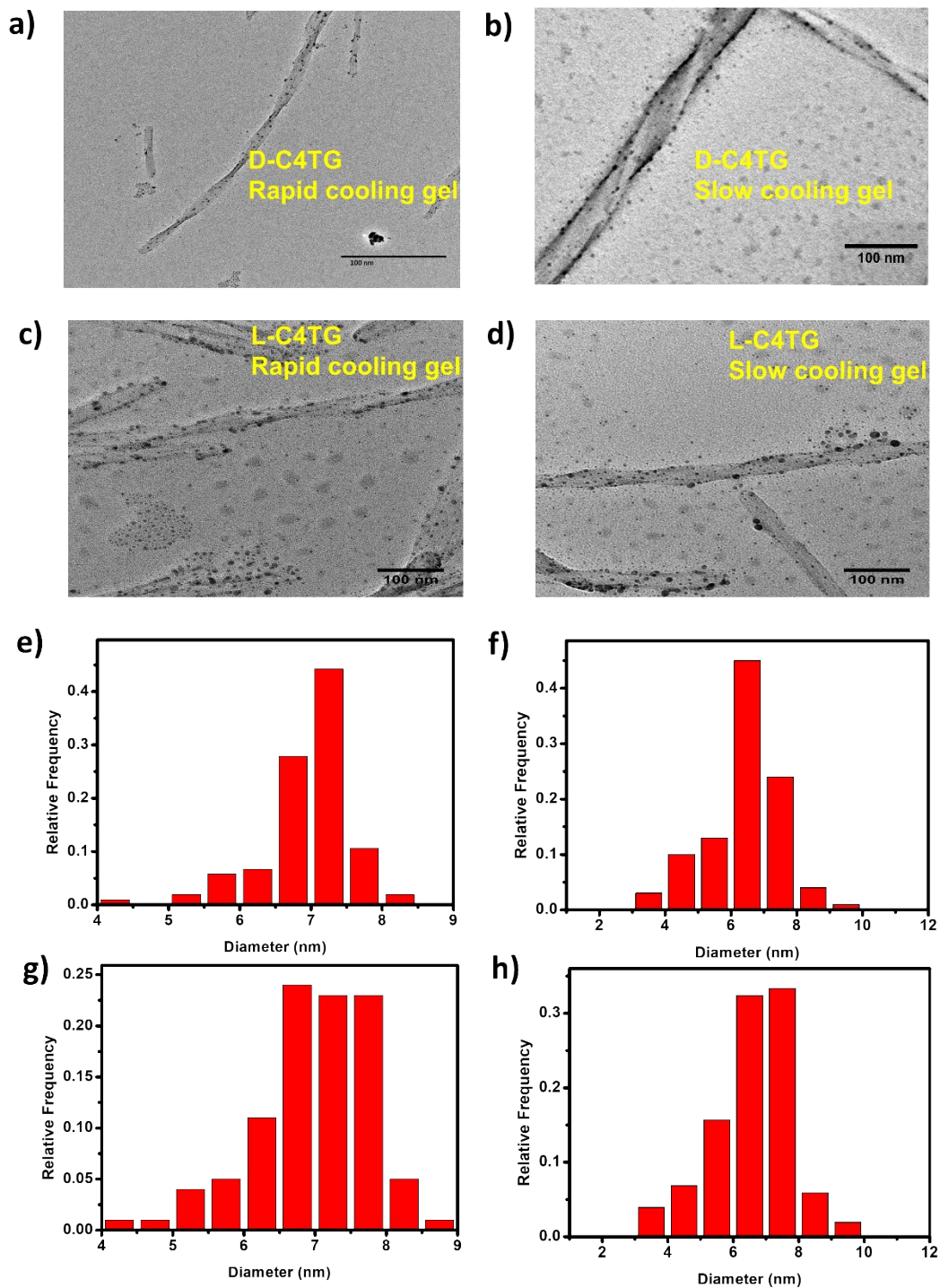


**Fig. S3** TEM images of D-C4TG hybrid material in RC process (a) and in SC process (b), and L-C4TG hybrid material in RC process (c) and in SC process (d) after UV irradiation. The corresponding histograms of the nanoparticles diameter (averaged over 100 nanoparticles) in RC process (e) and in SC process (f), and L-C4TG hybrid material in RC process (g) and in SC process (h) after UV irradiation.

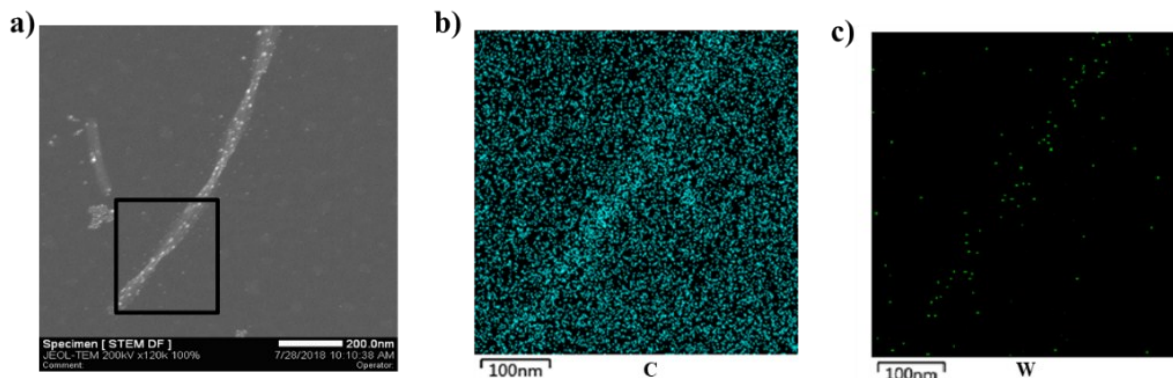


**Fig. S4** The elemental mapping of C (b) and W (c) hybrid after UV irradiation of D-C4TG hybrid material in RC process.

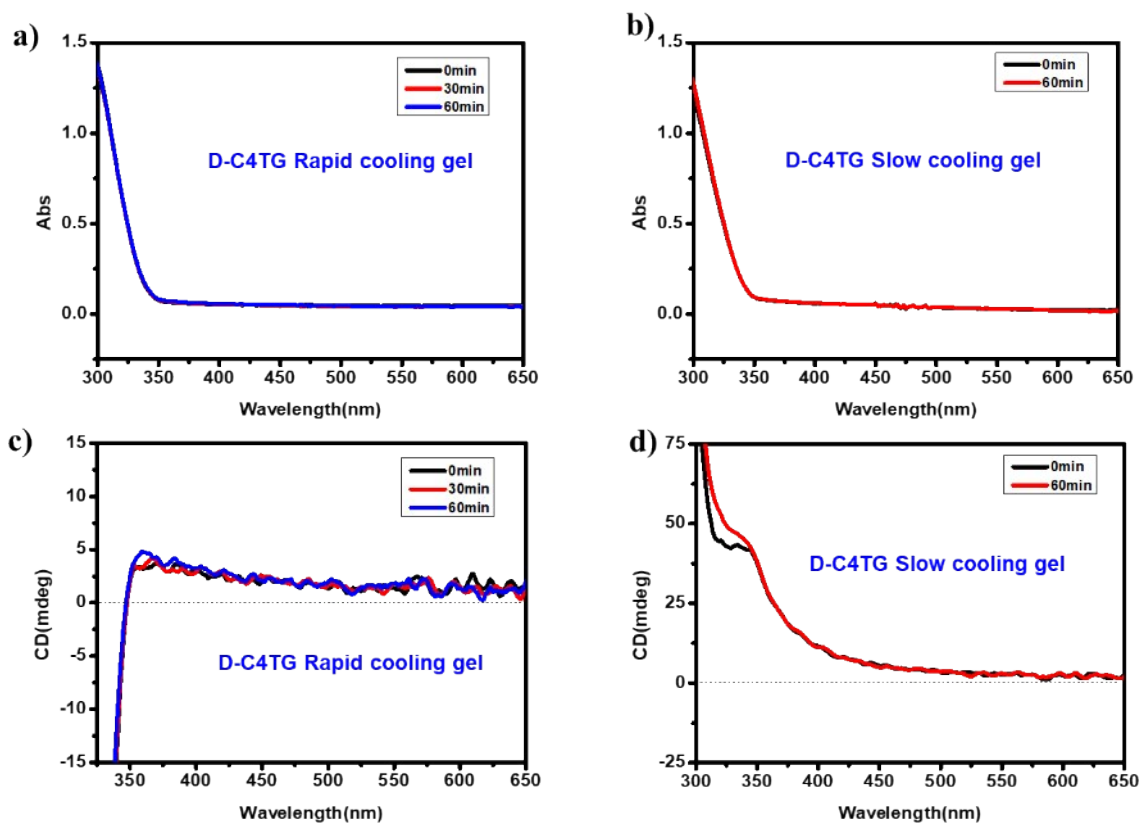


**Fig. S5** UV-Vis absorption spectra of D-C4TG hybrid material without  $[\text{SiW}_{12}\text{O}_{40}]^{4-}$  in RC process (a) and in SC process (b) after increasing durations of UV irradiation. CD spectra of D-C4TG hybrid material without  $[\text{SiW}_{12}\text{O}_{40}]^{4-}$  in RC process (c) and in SC process (d) after increasing durations of UV irradiation.

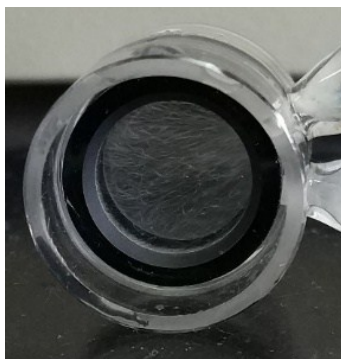


**Fig. S6** Picture of hybrid material containing equal parts of D-C4TG and L-C4TG gelator.

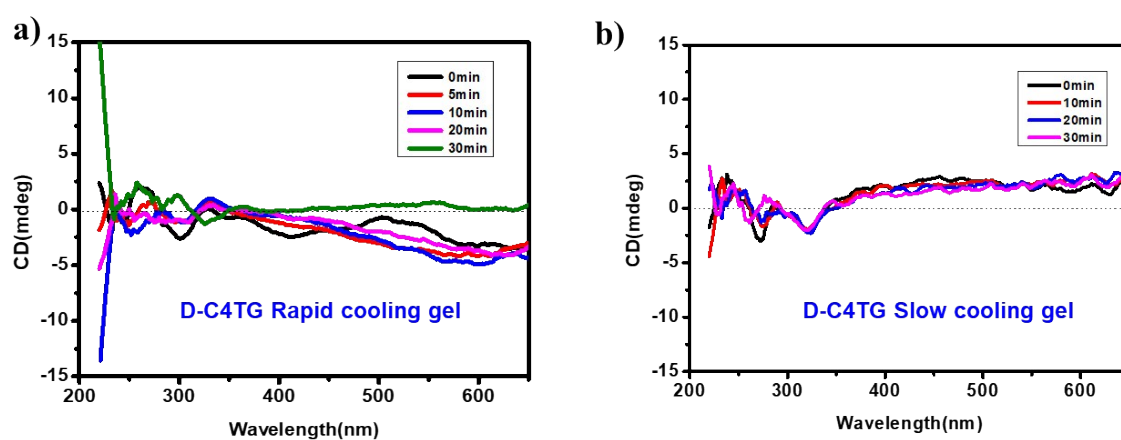


**Fig. S7** CD spectra of hybrid material containing equal parts of D-C4TG and L-C4TG gelator in RC process (a) and in SC process (b) after increasing durations of UV irradiation.

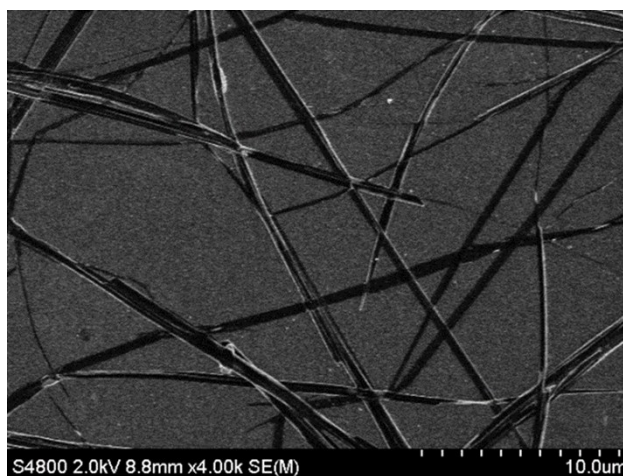


**Fig. S8** SEM image of hybrid material containing equal parts of D-C4TG and L-C4TG gelator.

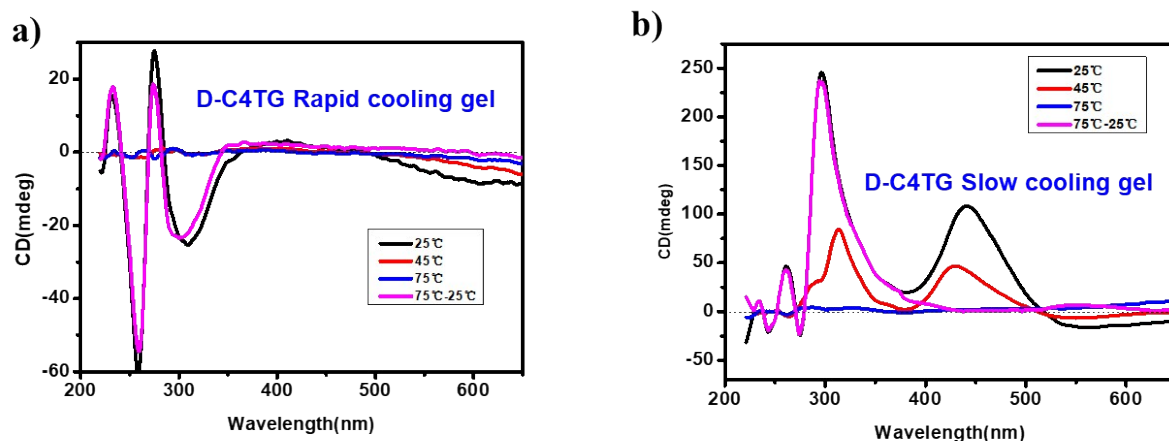


**Fig. S9** CD spectra of D-C4TG hybrid material in RC process (a) and in SC process (b) by heating the chiroptical hybrid material to 75°C when the chiral template gradually disappears.

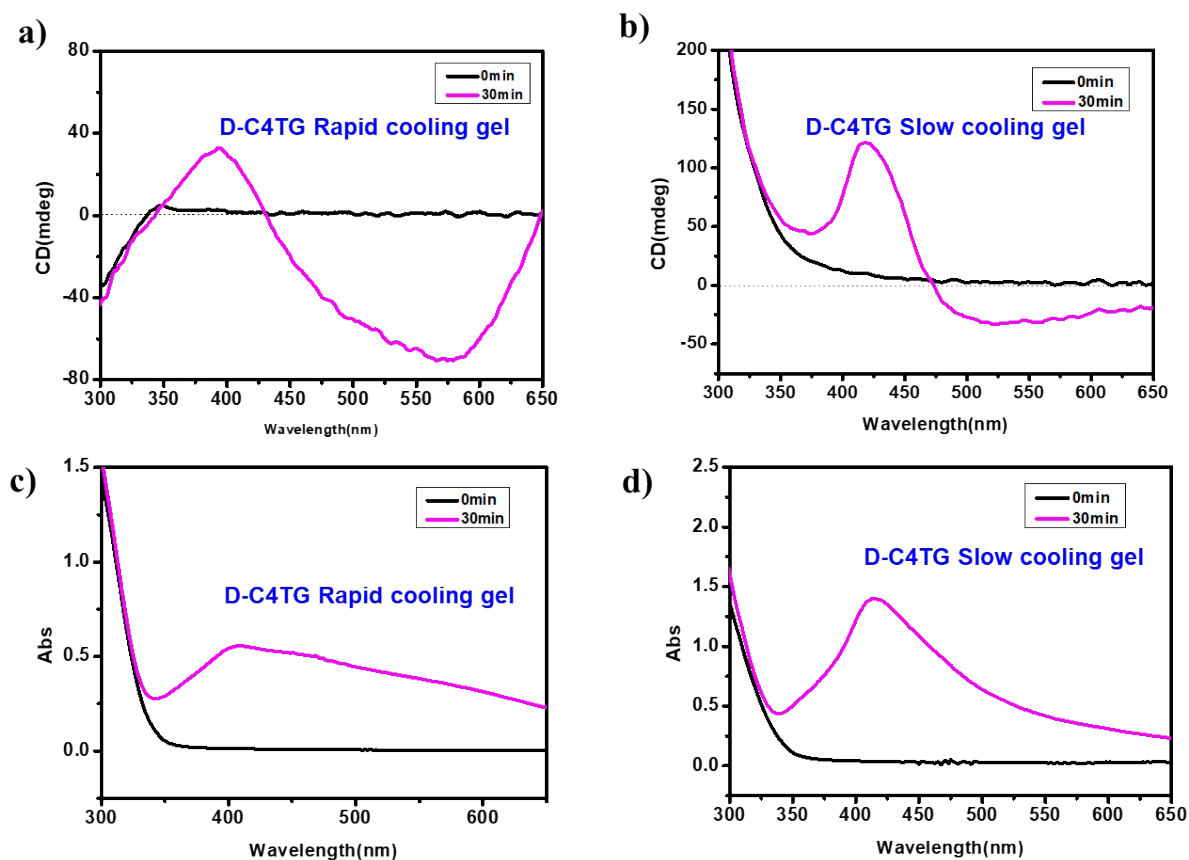


**Fig. S10** CD spectra of D-C4TG hybrid material in RC process (a) and in SC process (b) after UV irradiation 30min for C4TG/Ag<sup>+</sup> at the ratio of 1:1. UV-Vis absorption spectra of D-C4TG hybrid material in RC process (c) and in SC process (d) after UV irradiation 30min for C4TG/Ag<sup>+</sup> at the ratio of 1:1.

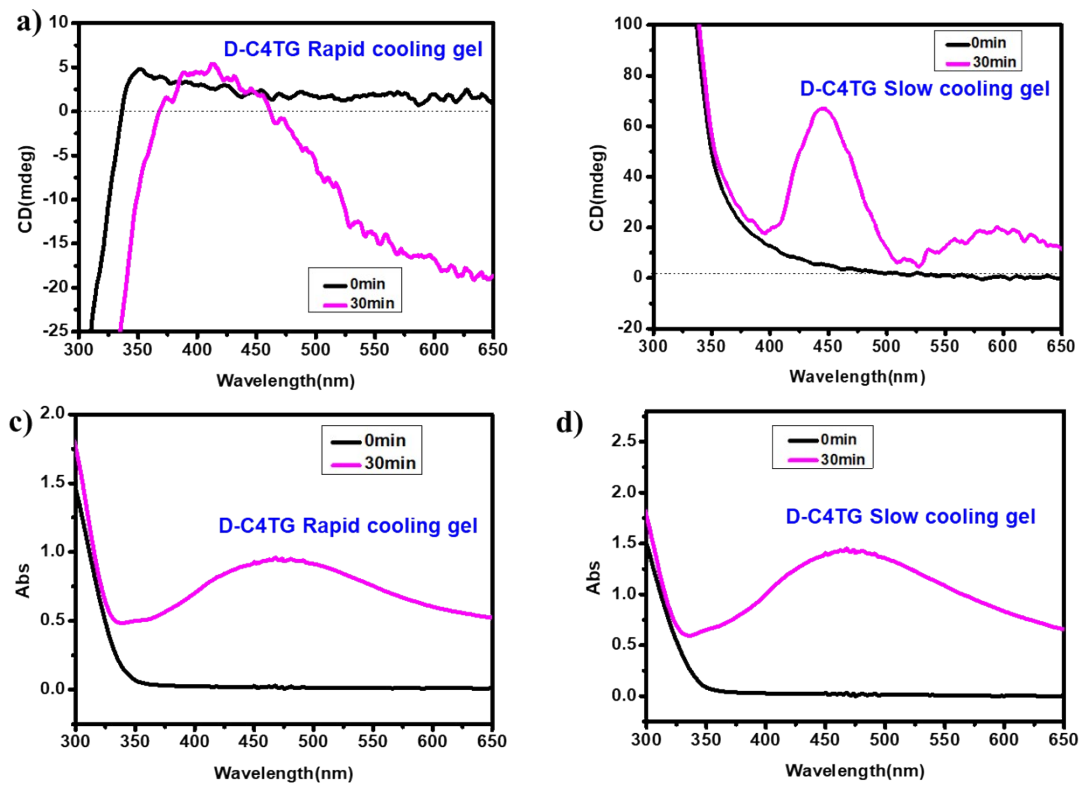


**Fig. S11** CD spectra of D-C4TG hybrid material in RC process (a) and in SC process (b) after UV irradiation 30min for C4TG/Ag<sup>+</sup> at the ratio of 1:20. UV-Vis absorption spectra of D-C4TG hybrid material in RC process (c) and in SC process (d) after UV irradiation 30min for C4TG/Ag<sup>+</sup> at the ratio of 1:20.



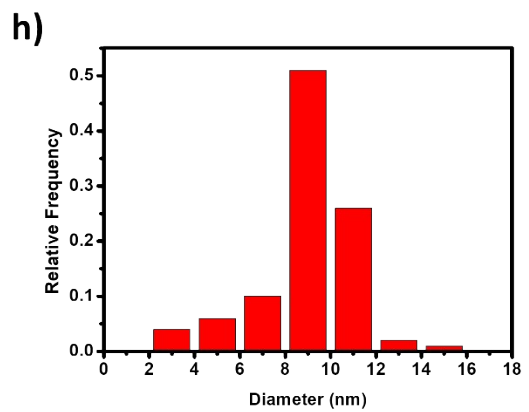
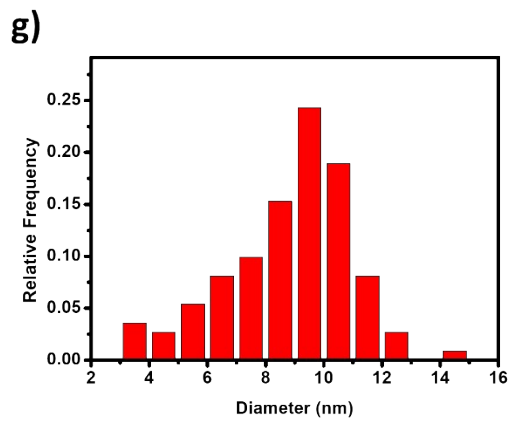
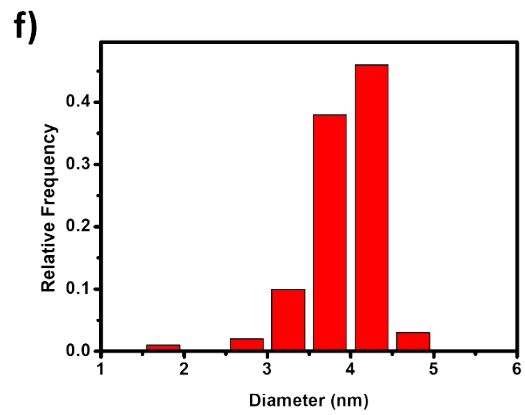
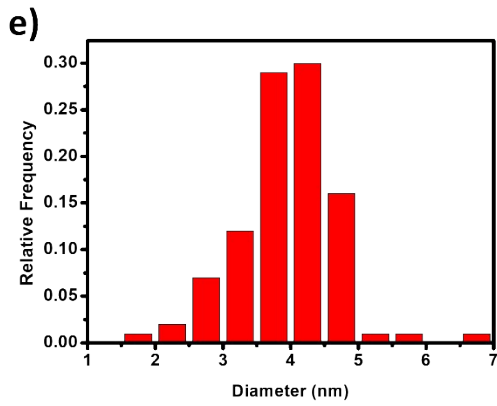
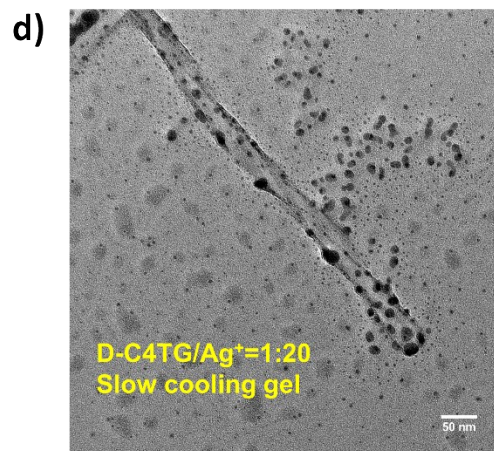
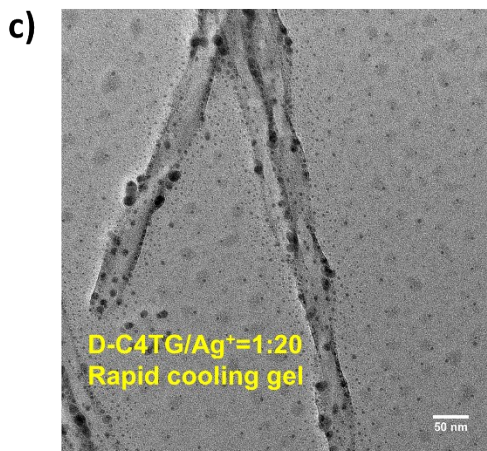
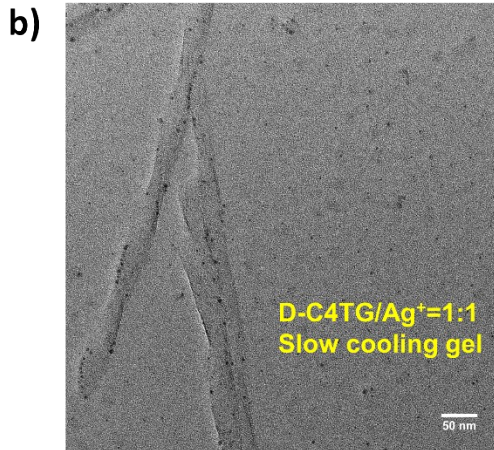
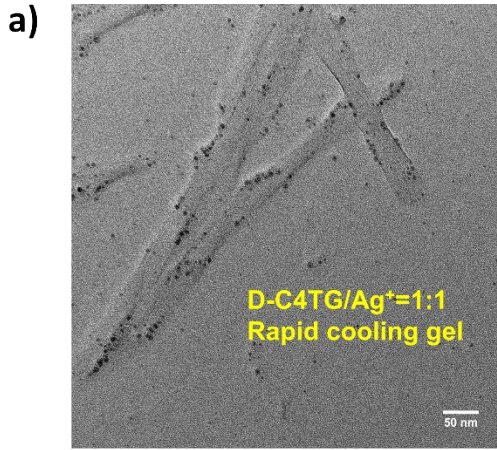


**Fig. S12** TEM images of hybrid material in RC process (a) and in SC process (b) for C4TG/Ag<sup>+</sup> at a ratio of 1:1 and hybrid material in RC process (c) and in SC process (d) for C4TG/Ag<sup>+</sup> at a ratio of 1:20 after UV irradiation for 30min. The corresponding histograms of the nanoparticles diameter (averaged over 100 nanoparticles) in RC process (e) and in SC process (f) for C4TG/Ag<sup>+</sup> at a ratio of 1:1 and hybrid material in RC process (g) and in SC process (h) for C4TG/Ag<sup>+</sup> at a ratio of 1:20 after UV irradiation for 30min.

## References

1 J. Cui, A. Liu, Y. Guan, J. Zheng, Z. Shen and X. Wan, *Langmuir*, 2010, **26**, 3615.